Surface energy induced patterning of organic and inorganic materials on heterogeneous Si surfaces

L. Tao, A. Crouch, F. Yoon, and B. K. Lee
Department of Electrical Engineering, University of Texas at Dallas, Richardson, Texas 75083

J. S. Guthi
Simmons Comprehensive Cancer Center, University of Texas Southwestern Medical Center, Texas 75390

J. Kim
Department of Electrical Engineering, University of Texas at Dallas, Richardson, Texas 75083

J. Gao
Simmons Comprehensive Cancer Center, University of Texas Southwestern Medical Center, Texas 75390

W. Hu[a)]
Department of Electrical Engineering, University of Texas at Dallas, Richardson, Texas 75083

(Received 10 June 2007; accepted 8 October 2007; published 6 December 2007)

A surface energy induced patterning (SEIP) method is developed to transfer resist patterns defined by lithography into various functional materials. A Si template is first chemically patterned using conventional lithography and selective attachment of trichlorosilane to achieve spatially different surface energies. Organic materials as well as inorganic films are deposited onto the chemically patterned template, followed by a thermal annealing process. The heterogeneous surface energies on the template induce material microfluidic reflow from the less to the more thermodynamically favorable areas. Using this method, patterned microstructures were achieved with SU-8, diblock copolymer, and aluminum film. In addition, the SEIP template was successfully used for atomic layer chemical vapor deposition to selectively pattern 200 nm–2 μm wide HfO_2 structures. © *2007 American Vacuum Society.* [DOI: 10.1116/1.2804577]

I. INTRODUCTION

The fabrication of nanostructures in functional polymers is of fundamental importance in exploiting nanotechnology for a wide range of applications,[1] including tissue engineering,[2] organic light emitting diodes,[3] polymer lasers,[4] organic solar cells,[5] polymer optics,[6,7] and nanomedicine.[8–10] State-of-the-art photolithography and e-beam lithography (EBL) are not feasible to directly pattern functional polymers because functional materials may not be sensitive to light or e-beam or their properties might be damaged during such exposure. Current semiconductor manufacturing processes use lithography to define patterns in resist, which is specially developed with high sensitivity and contrast to the light or e-beam radiation. A pattern transfer process is then used to transfer the resist patterns to the functional materials either by an etching or lift-off process.[11] This approach works fine for most materials, however, the etching step may affect the functionality of polymers such as those described below. Other innovative techniques such as nanoimprint lithography (NIL)[12] and soft lithography[13] can directly form nanostructures by molding the functional polymer. However, these processes result in a residual layer connecting the periodic polymer structures, which can be removed by an extra etching step. The etching step typically involves invasive chemicals or plasma which generally damage or change the functionality of materials. These processing issues of traditional lithography and imprinting techniques have posed limitations for the fabrication of functional polymer nanostructures and their applications.

Here a versatile pattern transfer process is developed to transfer lithographically defined resist patterns into functional materials using a surface energy induced patterning (SEIP) process. In the last decade, surface energy patterning or surface induced dewetting of polymers has been intensively researched both experimentally[14–19] and theoretically.[20–22] Similar dewetting behavior is also observed on metal thin films under laser radiation.[23,24] In addition, applied electric field or capillary forces can be used for better control of polymer self-assembly.[25,26] These studies have mostly focused on the polymer flow behaviors and are limited to a few polymer systems without functionality. The heterogeneous surface energies are typically formed by the selective binding of self-assembled monolayers (SAMs) to solid surfaces using soft lithography, which limits their resolution and accuracy at the submicron scale. Since the polymer dewetting process is not optimized, the uniformity and shape of the resulting polymer structures are relatively poor. The SEIP process here uses a molecular liftoff process to achieve good SAMs attachment to the Si surface.[27] Uniform gas pressure is used to improve polymer flow, resulting in uniform and well-controlled pattern morphology. Moreover, a variety of materials including SU-8, a popular material for microelectric-mechanic systems (MEMS), poly(ethylene glycol)-based block copolymers, and aluminum are demonstrated in the process. It was also used for vapor phase depo-

[a)]Electronic email: walter.hu@utdallas.edu

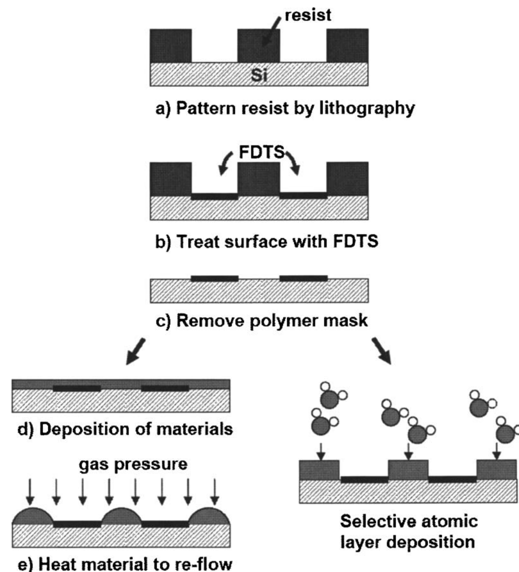

FIG. 1. Schematic illustration of the SEIP process utilizing both spin-on materials and ALD.

sition of high-*k* dielectrics HfO_2 using atomic layer deposition (ALD) in the areas of particular surface energy. The selective ALD of dielectrics can be used to make nanocapacitors or sensors. This method may allow more flexibility of fabrication for future nanotechnology products.

II. SEIP PROCESS

In the SEIP process, chemically patterned templates are used to induce spin-on material reflow and self-organization under thermal annealing and an applied gas pressure, resulting in discrete micro- and nanostructures on the surface. As shown in Fig. 1, conventional lithography, such as photolithography, nanoimprint, or EBL is used to define openings in the resist [Fig. 1(a)]. Then a trichlorosilane SAM, called (heptadecafluoro-1,1,2,2-tetrahydrodecyl) trichlorosilane (FDTS), is covalently bonded to the hydroxyl groups (OH–) on the surface of the Si openings [Fig. 1(b)]. After the resist removal, a Si template with heterogeneous surface energies is formed [Fig. 1(c)]. In other words, the hydrophilic Si–OH patterns are surrounded by the hydrophobic FDTS modified areas. Polymers are then spin coated or metal films are evaporated onto the Si templates [Fig. 1(d)]. Heating the deposited film at a temperature above the polymer glass transition temperature (T_g) or melting temperature (T_m) of metal allows the material to reflow and self-organize on the areas of high surface energy, leaving empty space at the areas of low surface energy [Fig. 1(e)].

For template making, 950 K poly(methyl methacrylate) (PMMA) was used for EBL and NIL. A reactive ion etching step with CF_4 chemistry was used to remove the residual layer of PMMA formed during NIL. S1813 resist was used for photolithography. The original Si sample was exposed to oxygen plasma to form uniform hydroxyl groups on the surface for later attachment of FDTS.[28] The surface energies of oxygen plasma treated Si and FDTS treated Si were measured as 72.6 and 17.8 mJ/m^2, respectively.[28] Various polymers with thicknesses of 80–600 nm were used in the experiments, including SU-8 and diblock copolymer of poly(ethylene glycol)-*b*-poly (D,L-lactide) (PEG-PLA). The PEG-PLA is a biocompatible polymer that has shown promising properties for advanced delivery of drugs and imaging agents.[29] It was synthesized by ring opening polymerization.[9] A gas pressure of 1–3 MPa was often applied above the film coated templates during the thermal annealing of material for better reflow. The SEIP experiments were performed on a hot plate as well as using an Obducat 2.5 nanoimprinter that provides precise control of temperature and gas pressure and results in higher yield. For SU-8 and PEG-PLA polymers, the annealing temperature was chosen to be between 70 and 100 °C, which is above their T_g of 40–50 °C. Under this annealing temperature, both polymers had a low enough viscosity to flow and form structures within a few minutes. In addition to polymer, 20 nm thick Al films were evaporated onto the SEIP templates. Annealing at a temperature of 700 °C for 10 min in an oven resulted in self-organization of Al patterns. The oven was filled with nitrogen during the annealing process to prevent the oxidation of Al.

Moreover, the SEIP template was used to induce site-specific ALD deposition of HfO_2, as shown in Fig. 1(f). The ALD process consisted of a 0.2/0.05 s for the Hf precursor/

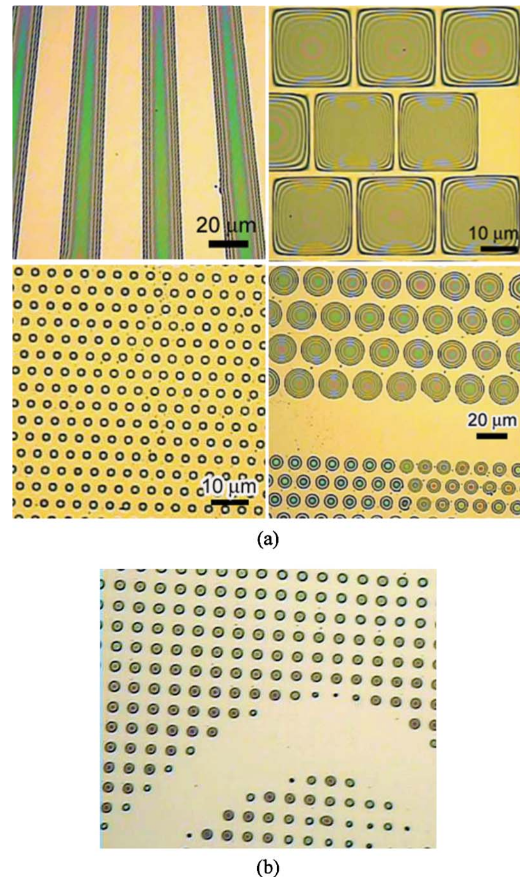

FIG. 2. (a) Optical images of the patterns in PEG-PLA diblock copolymer formed by the SEIP process at 100 °C for 10 min; (b) scratch test revealing residue-free polymer patterns.

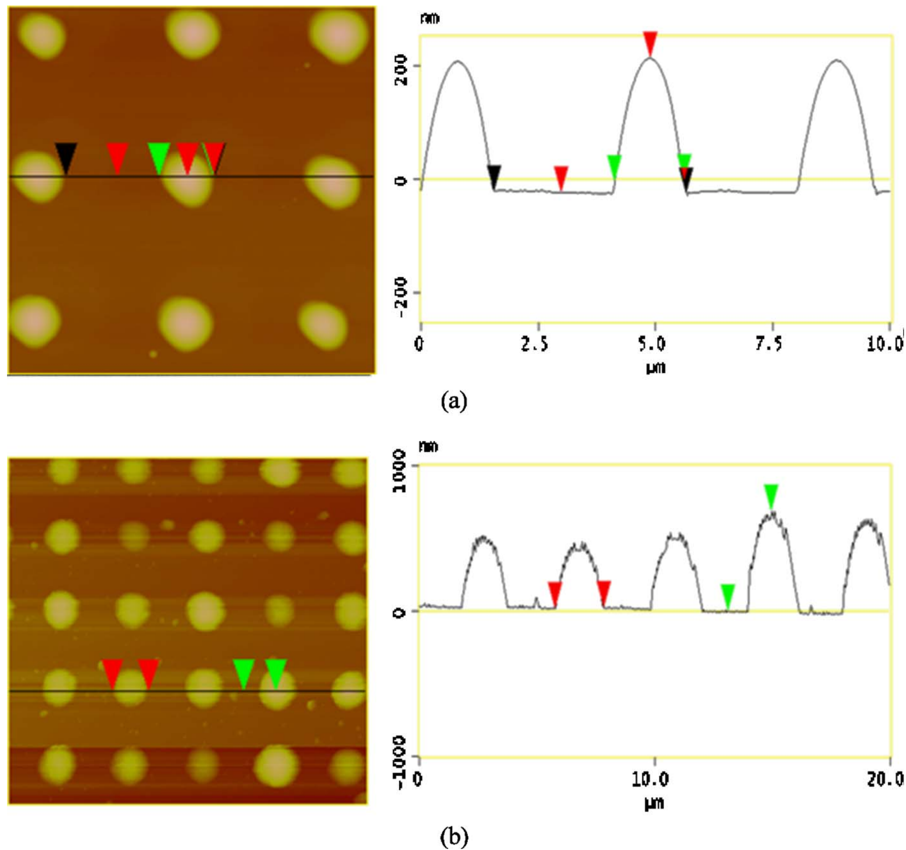

FIG. 3. AFM images and cross-sectional analysis of (a) SU-8 pillars, with a height of 235 nm and a diameter of ~2 μm and (b) PEG-PLA particles, with a height of 500–650 nm and a diameter of ~2 μm patterned by the SEIP process.

H_2O pulse time and 7 s of purging time with N_2. The temperatures of the substrate and the container of the of precursor were chosen to be 180 and 130 °C, respectively.

III. RESULTS

Figure 2(a) demonstrates the patterning of PEG-PLA copolymer into residue-free discrete microstructures without damaging its biofunctionality by heating the polymer-coated Si template to 100 °C. As displayed, this process has the flexibility to pattern a wide variety of structures including lines, pillars, holes, and squares with good uniformity and control. As described before, this process is advantageous for applications which require residue-free patterns. To confirm that no residue is present on the patterned template, a simple scratch test was conducted, as shown in Fig. 2(b). A blade scratch on the patterns indicates that there is no residual layer present. Optical images are capable of detecting thickness differences in the sub-10 nm range, further justifying this conclusion. This will allow the patterned polymer particles to release from the template and become suspended in an aqueous solution for medical applications, as demonstrated elsewhere.[30]

The atomic force microscopy (AFM) images in Fig. 3 characterize the morphology of the patterns and provide useful details. Figure 3(a) shows the spherical morphology of the 2 μm pillar array patterned in SU-8 with a much improved uniformity compared to previous similar studies.[16–19] The pillars show a height of approximately 235 nm and a pitch of 4 μm, indicating that the patterned SU-8 is indeed confined within the chemical patterns on the template. The spherical morphology which SU-8 displays is very uniform and the curvature is highly controllable, which can be used in producing microlenses for MEMS applications.

The patterns created in PEG-PLA are shown in Fig. 3(b). The structures range in height from approximately 500–650 nm and are measured to be 2.07 μm wide, which again closely matches the template dimensions. This particular sample does not display the same degree of uniformity displayed by SU-8. The uniformity of the pillars is affected by many factors including the initial film thickness, the uniformity of the film spin coating, as well as the polymer stability modes.[15] PEG-PLA contains a higher surface roughness after spin coating than does SU-8, allowing SU-8 to achieve better uniformity. Future studies will investigate more carefully the effect of initial film thickness on the pattern size, uniformity, and stability.

Figure 4 demonstrates patterns created by depositing both aluminum and high-K material HfO_2 by evaporation and ALD, respectively. A 20 nm layer of Al was deposited and annealed at 700 °C (T_m=660 °C), yielding well defined holes and pillars ranging from 1 to 20 μm in width. Additionally, the HfO_2 was deposited by ALD at a working pressure of 0.5 Torr on similar templates. HfO_2 only grew on the Si areas with high surface energy, with little deposition on the areas treated with FDTS. As a result, various residue-free structures are formed with high yield ranging from 200 nm to 2 μm in size with a pattern height of 10–40 nm, as shown in Figs. 4(b) and 4(c). The high deposition selec-

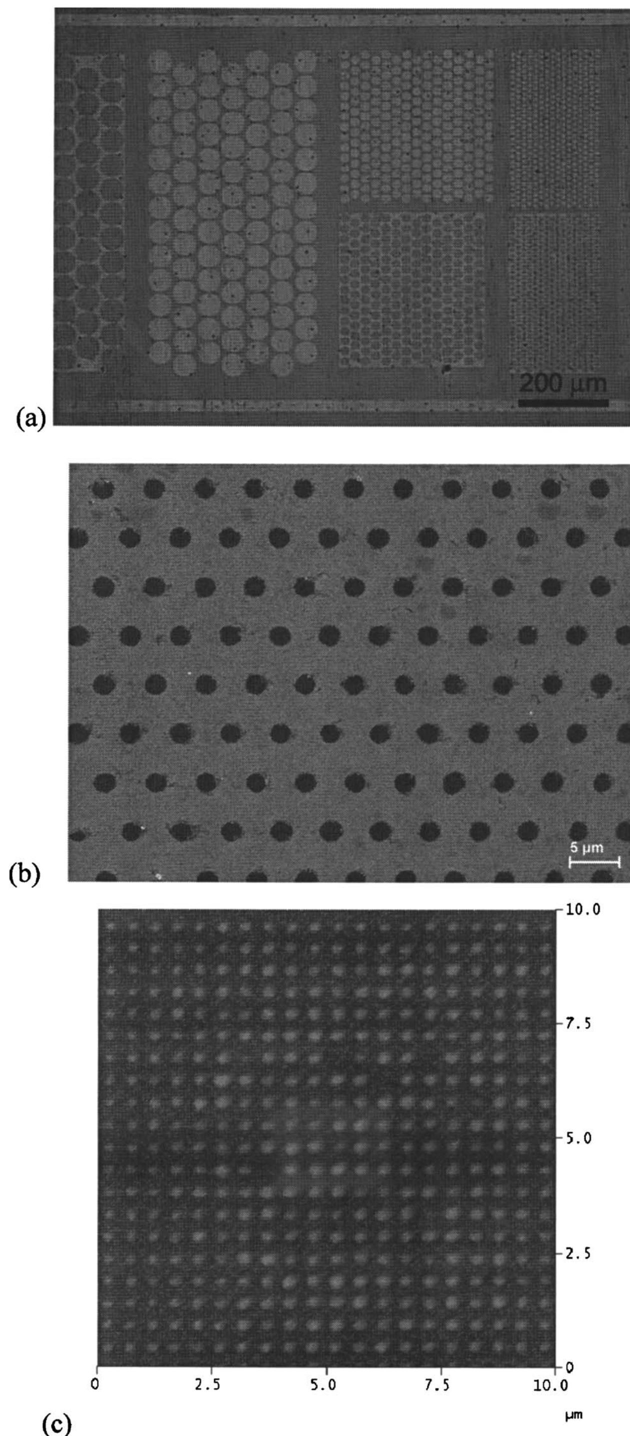

FIG. 4. (a) Al patterns ranging from 1 to 20 μm produced by SEIP at 700 °C for 10 min. Light areas are Al, dark areas are Si; (b) SEM image of 2 μm HfO_2 (dark color) patterns on Si (light areas); (c) AFM image of 200 nm HfO_2 pillar array with 500 nm pitch and 10 nm height.

tivity of the ALD process is likely due to the selective reaction between the hydroxyls on the surface and the Hf precursors.[31]

IV. DISCUSSION

The underlying science of SEIP is related to the different interfacial energies of the patterned materials with different surfaces. The interfacial free energy of the thin film at the FDTS coated Si and original Si–OH is very different. At the boundaries of Si–OH and FDTS patterns, a gradient of surface potential is formed and generates a pressure to drive thin film material flow from the less wettable areas (i.e., FDTS) to more wettable areas (i.e., Si–OH). Previously, ultrathin polymer films on homogeneous or heterogeneous surfaces were rigorously studied, determining that the van der Waals forces in the film and between the film and substrate were driving this migration of polymer to wettable areas.[11,16–19] However, because the film thickness is significantly higher in this case, the chemical pattern pitch is significantly smaller than the spinodal wavelength, leading us to believe that the pattern formation is due to the polymer viscous flow driven by the pressure at the heterogeneous boundaries of the template and not by the spinodal dewetting phenomena.[16–19] The measured contact angle of the SU-8 on the O_2 plasma treated Si surface is 69.2° [Fig. 3(a)], which is much higher than polymer typically coats Si at equilibrium according to Young's equation. This large contact angle indicates that the FDTS-Si boundary pressure is supporting the polymer structure, not allowing the polymer to relax into the FDTS area and assume its equilibrium position. This is similar to the observation of one-dimensional water channel formation reported previously.[15]

The patterning of Al using the SEIP process carries with it more complexity due to the high temperature which it requires. Heating the Si template and Al to a temperature of 700 °C should have two effects on the system. First, it is widely known that Al can diffuse into Si at temperatures as low as 350 °C.[32] This diffusion would suggest that the Al is not only present in the patterned areas, but perhaps also embedded in the Si and possibly on the hydrophobic areas. Additionally, the stability of the FDTS is also of concern at these temperatures. Many studies have been conducted to analyze how FDTS surface treatments react to high temperatures, finding that at temperatures around or above 500 °C, significant damage is done to the FDTS and the surface energy is thus altered considerably.[33] It is unknown how these two phenomena affect the SEIP process. Further studies will be conducted to characterize these two effects.

V. APPLICATIONS

The SEIP method provides a simple process to create periodic microscale and nanoscale patterns on solid surfaces. Since both organic and inorganic materials can be patterned with SEIP, wide applications are expected from electronic and optical devices to biomedical and nanomedicine systems, as shown in Fig. 5. For example, the additive patterning of HfO_2 patterns can be used for making electronic devices, such as capacitors. Also, with the future deposition of metals on top without any etching process, one can avoid etching induced defects or contaminations. SU-8 or other polymers can be patterned with perfect spherical morphology. By controlling the volume of the particles, the curvature can be precisely controlled. Therefore the spherical caps can work as micro- or nanolens with controlled numerical aper-

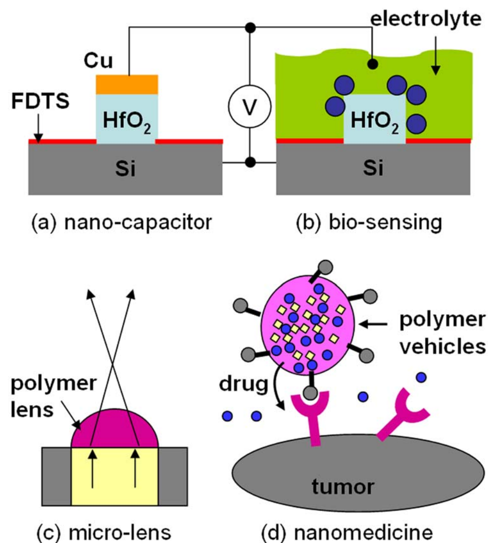

FIG. 5. Illustration of potential applications of SEIP method: (a) additive method to make capacitors for electronics; (b) capacitor or nanowire based biosensing; (c) polymer micro- or nanolens for MEMS; and (d) polymer drug-delivery vehicles for nanomedicine.

tures and focal length. These lenses can be integrated with prefabricated MEMS systems. The annealing temperature is about 60–100 °C, which allows for processing on plastic substrates.

Another major application area is the biomedical field, such as tissue engineering and nanomedicine. Biofunctional polymers or proteins can be patterned into periodic structures such as gratings and pillars which can affect cell adhesion and guide cell growth in a controlled manner. For nanomedicine applications, these particles will be lifted off from the surfaces. These free particles can work as vehicles for targeted delivery of drugs for chemotherapy or contrast agents for bioimaging.

VI. SUMMARY

A surface energy induced self-assembly method has been established to pattern uniform and high quality microstructures in functional materials. The boundary gradient of interfacial potential is the driving force for material self-organization. The uniformity of the resulting patterns is related to the uniformity of the initial deposited material, as well as the initial film thickness. Using SEIP, the patterning of epoxy polymer, diblock copolymer, aluminum, and HfO_2 dielectric materials is achieved with well-controlled morphology and dimensions. The SEIP process shows potential for a wide range of applications in semiconductor and nanotechnology areas.

ACKNOWLEDGMENTS

The authors would like to thank Stella W. Pang at the University of Michigan for her support on some of the mold fabrication. They also thank Moon Kim and Heather Hillebrenner for useful discussion. This work is supported in part by Moncrief Foundation, the Texas Higher Education Coordinating Board through Advanced Research Program under Contract No. 009741-0015-2006 to one of the authors (W.H.) and a NIH grant (R21 EB005394) to another author (J.G.). Two of the authors (J.K. and B.I.) also acknowledge a partial financial support from the "Center for Nanostructured Materials Technology" (Code No. M105KO010026-05K1501-02611) through the Ministry of Science and Technology, Korea.

[1]L. J. Guo, Adv. Mater. (Weinheim, Ger.) **19**, 495 (2007).
[2]W. Hu, E. Yim, R. M. Reano, K. W. Leong, and S. W. Pang, J. Vac. Sci. Technol. B **23**, 2984 (2005).
[3]A. Bolognesi, C. Botta, and S. Yunus, Thin Solid Films **492**, 307 (2005).
[4]E. Mele, A. Camposeo, R. Stabile, P. D. Carro, F. D. Benedetto, L. Persano, R. Cingolani, and D. Pisignano, Appl. Phys. Lett. **89**, 131109 (2006).
[5]M. S. Kim, J. S. Kim, J. C. Cho, M. Shtein, L. J. Guo, and J. Kim, Appl. Phys. Lett. **90**, 123113 (2007).
[6]Y. Huang, G. T. Paloczi, A. Yariv, C. Zhang, and L. R. Dalton, J. Phys. Chem. B **108**, 8606 (2004).
[7]M. B. Christiansen, M. Scholer, and A. Kristensen, Opt. Express **15**, 3931 (2007).
[8]N. A. Peppas, MRS Bull. **31**, 888 (2006).
[9]N. Nasongkla, E. A. Bey, J. Ren, H. Ai, C. Khemtong, J. G. Setti, S. F. Chin, A. D. Sherry, D. A. Boothman, and J. Gao, Nano Lett. **6**, 2427 (2006).
[10]G. B. Sukhorukov and H. Mohwald, Trends Biotechnol. **25**, 93 (2007).
[11]J. Plummer, M. Deal, and P. Griffin, *Silicon VLSI Technology* (Prentice Hall, Englewood Cliffs, NJ, 2000).
[12]S. Y. Chou, P. R. Krauss, and P. J. Renstrom, J. Vac. Sci. Technol. B **14**, 4129 (1996).
[13]Y. Xia and G. M. Whitesides, Annu. Rev. Mater. Sci. **28**, 153 (1998).
[14]A. M. Higgins and R. A. L. Jones, Nature (London) **404**, 476 (2000).
[15]H. Gau, S. Herminghaus, P. Lenz, and R. Lipowsky, Science **283**, 46 (1999).
[16]M. Woodson and J. Liu, Phys. Chem. Chem. Phys. **9**, 207 (2007).
[17]X. J. Wang, M. Ostblom, T. Johansson, and O. Inganas, Thin Solid Films **449**, 125 (2004).
[18]J. Z. Wang, Z. H. Zheng, H. W. Li, W. T. S. Huck, and H. Sirringhaus, Nat. Mater. **3**, 171 (2004).
[19]D. Julthongpiput, W. Zhang, J. F. Douglas, A. Karim, and M. J. Fasolka, Soft Matter **3**, 613 (2007).
[20]M. Sferrazza, M. Heppenstall-Butler, R. Cubitt, D. Bucknall, J. Webster, and R. A. L. Jones, Phys. Rev. Lett. **81**, 5173 (1998).
[21]C. Redon, F. Brochard-Wyart, and F. Rondelez, Phys. Rev. Lett. **66**, 715 (1991); R. Xie, A. Karim, J. F. Douglas, C. C. Han, and R. A. Weiss, *ibid.* **81**, 1251 (1998).
[22]K. Kargupta and A. Sharma, Phys. Rev. Lett. **86**, 4536 (2001).
[23]J. Bischof, D. Scherer, S. Herminghaus, and P. Leiderer, Phys. Rev. Lett. **77**, 1536 (1996).
[24]A. Favazza, R. Kalyanaraman, and R. Sureshkumar, Nanotechnology **17**, 4229 (2006).
[25]S. Y. Chou and L. Zhuang, J. Vac. Sci. Technol. B **17**, 3197 (1999).
[26]A. M. Bruinink, M. Peter, P. A. Maury, M. De Boer, M. L. Kuipers, J. Huskens, and D. N. Reinhoudt, Adv. Funct. Mater. **16**, 1555 (2006).
[27]K. Sarveswaran, W. Hu, P. Huber, G. H. Bernstein, M. Niemier, and M. Lieberman, Langmuir **22**, 11279 (2006).
[28]W. Hu, B. Yang, C. Peng, and S. W. Pang, J. Vac. Sci. Technol. B **24**, 2225 (2006).
[29]D. Sutton, N. Nasongkla, E. Blanco, and J. Gao, Pharm. Res. **24**, 1029 (2007).
[30]W. Hu, F. Yoon, A. Crouch, L. Tao, H. Hillebrenner, J. S. Guthi, M. Kim, and J. Gao, IEEE Trans. Nanotechnol. (submitted).
[31]R. Chen, H. Kim, P. McIntyre, D. Porter, and S. Bent, Appl. Phys. Lett. **86**, 191910 (2005).
[32]K. Nakamura and M. Kamoshida, J. Appl. Phys. **48**, 5349 (1977).
[33]Y. X. Zhuang *et al.*, J. Micromech. Microeng. **16**, 2259 (2006).

View publication stats